

Natural Products

International Edition: DOI: 10.1002/anie.201709720
German Edition: DOI: 10.1002/ange.201709720Crochelins: Siderophores with an Unprecedented Iron-Chelating Moiety from the Nitrogen-Fixing Bacterium *Azotobacter chroococcum*

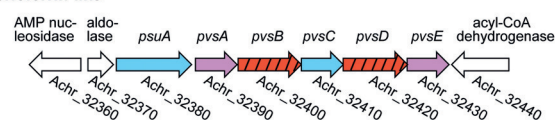
Oliver Baars, Xinning Zhang, Marcus I. Gibson, Alan T. Stone, François M. M. Morel, and Mohammad R. Seyedsayamdost*

Abstract: Microbes use siderophores to access essential iron resources in the environment. Over 500 siderophores are known, but they utilize a small set of common moieties to bind iron. *Azotobacter chroococcum* expresses iron-rich nitrogenases, with which it reduces N_2 . Though an important agricultural inoculant, the structures of its iron-binding molecules remain unknown. Here, the “chelome” of *A. chroococcum* is examined using small molecule discovery and bioinformatics. The bacterium produces vibrioferrin and amphibactins as well as a novel family of siderophores, the crochelins. Detailed characterization shows that the most abundant member, crochelins, binds iron in a hexadentate fashion using a new iron-chelating γ -amino acid. Insights into the biosynthesis of crochelins and the mechanism by which iron may be removed upon import of the holo-siderophore are presented. This work expands the repertoire of iron-chelating moieties in microbial siderophores.

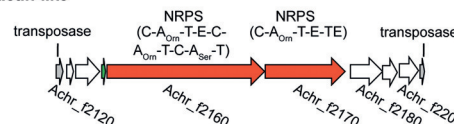
Iron is an essential micronutrient for nearly all life forms, and its limited solubility under ambient conditions has led to a number of strategies for acquiring, monopolizing, and pirating it.^[1] Micro-organisms typically utilize siderophores, a group of secondary metabolites that bind iron with staggering affinity and deliver the bound ferric iron to the cell.^[2] To date, over 500 siderophores have been discovered,^[1] a process that has been facilitated by their well-understood biological activity and, recently, by genome mining approaches.^[1,3] While the structures of the siderophores elucidated thus far are diverse, the iron-chelating groups are limited to a combination of catechols, *o*-hydroxyphenyl-oxazolines, hydroxamates, α -hydroxycarboxylates, α -amino-carboxylates, and in rare cases, α -hydroxyimidazoles.^[1] Herein, we report the structure of a siderophore with an unprecedented iron-chelating moiety from the γ -proteobacterium *Azotobacter chroococcum*.

A. chroococcum is a free-living, nitrogen-fixing bacterium that is commonly found in soil, water, the rhizosphere, and phyllosphere.^[4,5] It has been used as an agricultural inoculant, owing to its ability to stimulate plant growth via nitrogen fixation and the synthesis of plant hormones.^[6–8] Despite its importance and widespread use in agriculture, however, its secondary metabolome is largely unknown. Structures of siderophores have not yet been reported from *A. chroococcum*, and how this bacterium gains access to iron, which it requires to generate high concentrations of nitrogenases, remains to be determined. A bioinformatic search in the recently sequenced genome of *A. chroococcum*^[5] reveals three siderophore gene clusters, possibly leading to the production of vibrioferrin (Figure 1a), amphibactin (Figure 1b), and an unknown metallophore (Figure 1c). To gain insights into the products of these gene clusters, we employed our recently reported workflow for uncovering the chelome of *A. chroococcum*, that is, the secondary metabolites that it

a vibrioferrin-like



b amphibactin-like



c unidentified putative siderophore

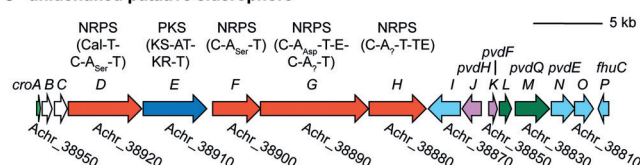


Figure 1. Identifiable siderophore biosynthetic gene clusters in *Azotobacter chroococcum*. Bioinformatic searches identify clusters similar to those reported for vibrioferrin (a) and amphibactin (b). A third cluster, *cro*, is also shown, without sequence homology to those of known siderophores (c). Gene color codes: non-ribosomal peptide synthetases (NRPSs), red; NRPS-independent siderophore synthetases, red stripes; polyketide synthase (PKS), blue; genes involved in the synthesis of precursors, purple; metabolite transporters, light blue; deacylases, green; *mbtH*, light green; genes of unknown/difficult-to-predict functions, white. Unique locus tags are shown for each gene. For the NRPSs and PKS, the predicted domain arrangements and adenylation (A) domain specificities are indicated. The *cro* cluster contains a number of genes orthologous to those in the pyoverdine (*pvd*) gene cluster.

[*] Dr. O. Baars, Prof. Dr. X. Zhang, Prof. Dr. F. M. M. Morel
Department of Geosciences, Princeton University
Princeton, NJ 08544 (USA)

Dr. M. I. Gibson, Prof. Dr. M. R. Seyedsayamdost
Department of Chemistry, Princeton University
Princeton, NJ 08544 (USA)
E-mail: mrseyed@princeton.edu

Prof. Dr. A. T. Stone
Department of Environmental Health and Engineering
Johns Hopkins University
Baltimore, MD 21218 (USA)

Supporting information and the ORCID identification number(s) for the author(s) of this article can be found under:
<https://doi.org/10.1002/anie.201709720>.

synthesizes to acquire iron and other transition metals from the environment.^[9,10] In this method, the bacterium is cultured in iron-limited and iron-replete media, and the resulting supernatants are subjected to solid-phase extraction, high-resolution (HR)-HPLC-MS, and HR-MS/MS. The data are then computationally assessed, using the mass isotopes of iron, to provide a picture of all the siderophores that the organism can biosynthesize.^[9,10] The results of this workflow applied to *A. chroococcum* allowed us to identify three distinct groups of iron-binding metabolites (Figure 2; Supporting Information, Figure S1). Two of these were in the vibrioferrin^[10] and amphibactin^[11] class of siderophores, in line with our bioinformatic analyses (Figure 1; Supporting Information, Table S1). The third, the focus of this report, is a novel siderophore that we call crochelin (Figure 2).

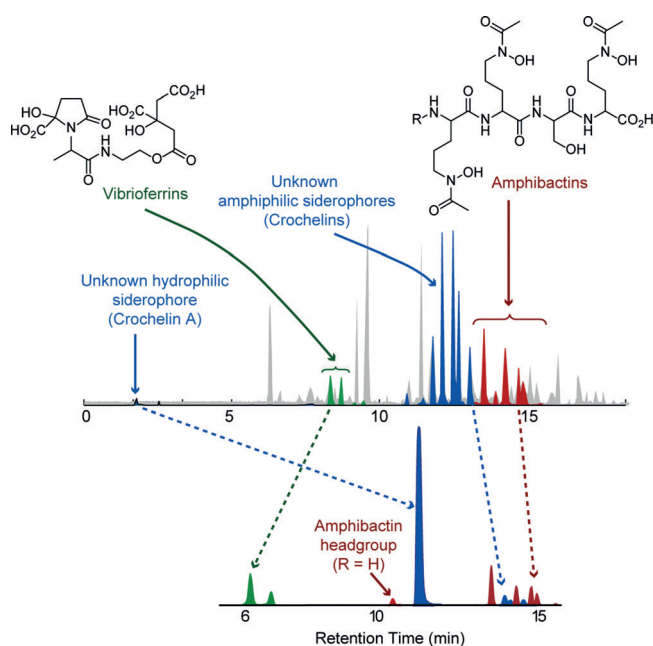


Figure 2. Identification of iron-binding metabolites from supernatants of *A. chroococcum* cultures. Top: Our workflow identifies three groups of iron-binding metabolites, belonging to the vibrioferrin (green peaks) and amphibactin (red) classes, as well as a third, new group, crochelin (blue). Note that different amphibactin peaks represent various acyl chains as the R group. Bottom: Quantification of siderophores via direct HPLC-MS injection (without solid-phase extraction) with an added ion-pairing reagent (heptafluorobutyric acid) as mobile phase buffer. The new hydrophilic siderophore, crochelin A, is the most abundant peak.

To elucidate the structure of crochelin, we generated large-scale *A. chroococcum* production cultures and isolated several crochelin analogues, which were then analyzed by 1D/2D NMR (Figure 3a; Supporting Information, Figures S2–S19). For the most abundant variant, the hydrophilic crochelin A (**1**), ¹H, COSY, and TOCSY spectra revealed an amino acid backbone and a total of six spin systems, with identifiable α -proton resonances at 4.38, 4.60, 4.37, and 4.10 ppm (Supporting Information, Figures S2–S4). Using HSQC and HMBC data, the spin systems were identified as the canonical amino acid Ser and five non-canonical units comprised of β -

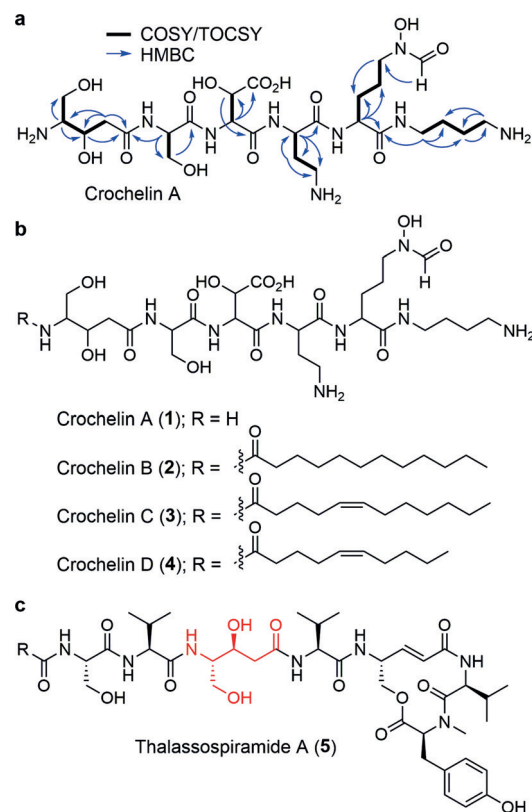


Figure 3. Crochelins, a new class of siderophores. a) Relevant NMR correlations used to solve the structure of crochelin A, the most abundant variant. b) Structures of crochelin A and acylated derivatives, crochelin B–D. c) Structure of thalassospiramide A, representative of the only other group of metabolites with the unusual ADPA moiety, which is shown in red.

hydroxyaspartic acid (β -OH-Asp), diaminobutyric acid (Dab), *N*-formyl-*N*-hydroxyornithine (*N*-formyl-*N*-OH-Orn), an acylated putrescine, and the unusual γ -amino acid 4-amino-3,5-dihydroxypentanoic acid (ADPA) (Figure 3b; Supporting Information, Figures S5–S7). This latter monomer has only been observed in one other natural product, the non-siderophore immuno-suppressant thalassospiramide^[12] (**5**, Figure 3c). The identities of these residues were further verified by HR-MS/MS, which revealed all b and most y ions at each peptide bond, with the fragment *m/z* values entirely consistent with the six monomers elucidated by NMR. The sequence of **1** was also derived from HR-MS/MS (Supporting Information, Figure S20, Tables S2, S3) and verified by NMR analysis: HMBC correlation from the putrescine spin system, specifically the amide-adjacent methylene group ($\delta_{\text{H}} = 3.07$) to the carbonyl carbon of the C-terminally modified Orn ($\delta_{\text{C}} = 173.3$), verified the site of attachment. Additional HMBC correlations along the peptide backbone were in agreement with the sequence derived from HR-MS/MS, thus completing the two-dimensional structure of **1** (Supporting Information, Tables S3, S4).

We also solved the structures of three minor variants, crochelins B–D (**2–4**, Figure 3b; Supporting Information, Figures S8–S19, Table S5). HR-MS data showed **2** to contain a saturated acyl group, while the acyl chains in **3** and **4** were

unsaturated (Supporting Information, Figures S21, S22, Table S2). For crochelin B, ^1H and ^{13}C chemical shifts, NOESY correlations from the acyl group to the ADPA moiety, as well as HR-MS/MS revealed the *N*-terminus of crochelin A as the site of attachment of the acyl group. **3** and **4** contained unsaturated acyl groups also at the *N*-terminus; the location and geometry of unsaturation in **3** and **4** were determined by 1D/2D NMR analysis (Supporting Information, Table S5). Together, we were able to solve the structures of four crochelins. The most abundant (**1**), bears a free *N*-terminus, whereas three relatively minor components carry diverse acyl chains. Based on HPLC-MS analysis, > 90 % of crochelins are present as variant A, while the remaining acylated derivatives make up < 10 % (Figure 2, bottom).

Crochelins represent a new class of putative metal-lophores with a rare ADPA moiety. They share substructures with malleobactin^[13] and ornibactin,^[14] specifically the acylated putrescine as well as *N*-formyl-*N*-OH-Orn and β -OH-Asp, but differ in the Dab and ADPA moieties. With the structures of crochelins characterized, we next sought to assess their roles as bona fide siderophores, the function of the ADPA substructure in chelating iron, as well as their biosynthesis. To test whether crochelin is a genuine siderophore, we examined its production as a function of the total concentration of ferric iron, $[\text{Fe}^{\text{III}}]$. We observed a clear dependence of the levels of **1** on $[\text{Fe}^{\text{III}}]$ in the growth medium (Figure 4a; Supporting Information, Table S6). Optimal production of **1** was observed in iron-limited media, while little to no crochelin production was detected in cultures supplemented with > 5 μM Fe^{III} . These results strongly suggest that *A. chroococcum* synthesizes **1** in response to iron limitation and therefore utilizes it as a siderophore.

Crochelin A contains two well-known iron-chelating groups, a hydroxamate and an α -hydroxycarboxylate (α -OH-CO₂H). It could bind Fe^{III} in an uncommon, weak tetradentate fashion.^[1] Alternatively, binding via ADPA could provide tight hexadentate chelation of Fe^{III} . We first examined the mode of iron binding structurally, but repeated attempts to crystallize Fe^{III} -complexed **1** failed. We subsequently used HR-MS, pFe measurements, cyclic voltammetry (CV), and UV/Vis spectroscopy to examine the role of ADPA in binding Fe^{III} .

Tetradentate siderophores can form a 3:2 complex with iron, thus enabling hexadentate ligation.^[1] HR-MS analysis of Fe^{III} -crochelin A showed that this was not the case and that the complex consisted of a 1:1 siderophore/iron ratio, consistent with hexadentate binding (Supporting Information, Figure S20). We further differentiated between these options by determining the tightness of iron binding via pFe measurements. pFe is the negative logarithm of free, aqueous Fe^{III} at fixed concentrations of siderophore, iron, and H^+ (pH). The tighter a given siderophore binds iron, the higher its pFe. Reported pFe values show that hydroxamate chelation is stronger than that by α -OH-CO₂H (Supporting Information, Table S7). For example, the pFe of ferrioxamines with 3 hydroxamates is about 25–27.^[1] The pFe value of aerobactin, a hexadentate siderophore with 2 hydroxamates and an α -OH-CO₂H is 23.4. A tetradentate siderophore with 2 hydroxamates, rhodotorulic acid, exhibits a pFe of 22,

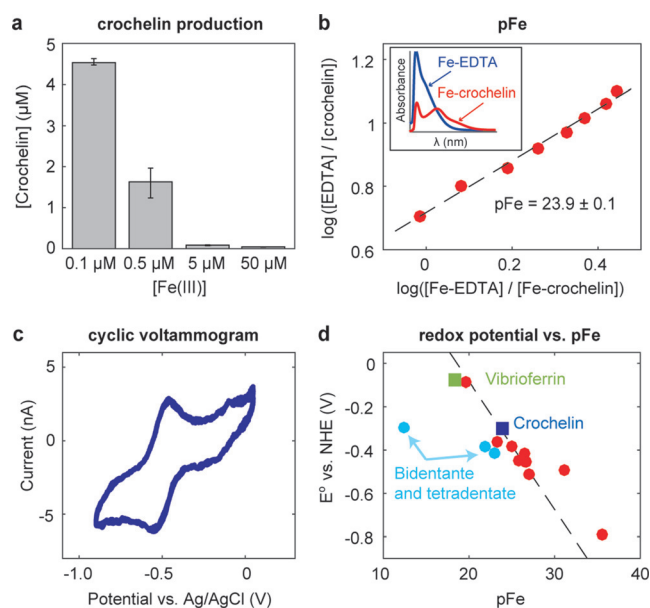


Figure 4. Crochelin A is a bona fide, hexadentate siderophore. a) Quantification of the levels of **1** as a function of $[\text{Fe}^{\text{III}}]$ in *A. chroococcum* cultures. b) Determination of pFe for **1** using EDTA competition assays. Inset: absorption spectra of Fe^{III} -EDTA (blue trace) and Fe^{III} -crochelin A (red trace). c) Determination of the reduction potential of Fe^{III} -crochelin A by CV yields a value of -0.28 V (vs. NHE) at pH 7.4. d) Plot of E° vs. pFe for **1** and other siderophores. The dotted line describes the observed trend for hexadentate siderophores (red circles) with a slope of 59.2 mV/pFe. Bidentate and tetradentate siderophores are shown in blue circles. Vibrioferriin (green square) and **1** (blue square) are marked. See the Supporting Information, Table S7 for details.

that is, it binds iron 10^3 – 10^5 -fold weaker than ferrioxamine. Using standard assays, we determined a pFe value of 23.9 for **1** (Figure 4b; Supporting Information, Figure S23), similar to that for aerobactin. Interestingly, the *N*-acylated crochelin D exhibited a lower pFe. The measurements were complicated by the low solubility of **4**, but our assays showed that its pFe was significantly lower than 23.4, the pFe of EDTA (Supporting Information, Figure S24). These measurements strongly suggest that **1** binds Fe^{III} in a hexadentate fashion via its hydroxamate, α -OH-CO₂H, and ADPA groups. Acylation of the ADPA-amine led to a significant reduction in the pFe, suggesting that the terminal amine and one or both hydroxy groups in ADPA are involved in binding Fe^{III} .

We acquired UV/Vis absorption spectra as a function of pH to further assess iron binding in **1**, and observed a shift between pH 5.5 and 4 (Supporting Information, Figure S25). In contrast, the absorption spectra of ferrioxamine B (FOB), remain unchanged in that pH range, indicating the spectral shifts of **1** are associated with α -OH-CO₂H and/or ADPA. With **4**, the UV/Vis spectrum changes between pH 7.4 and 5.5, with the features differing from those of **1** (Supporting Information, Figure S25). While we cannot ascribe the spectral features to specific transitions, the disparate pH-dependence of the UV/Vis spectra supports differential Fe^{III} -binding in **1** vs. **4** and FOB, again implicating the ADPA group in iron ligation.

Additional evidence for this conclusion came from electrochemical studies on Fe^{III}-crochelin A. Analysis of standard reduction potentials (E°) of a wide variety of Fe^{III}-complexed siderophores show clear and disparate trends for tetradentate and hexadentate siderophores. CV studies with Fe^{III}-**1** showed a single redox couple with a reversible CV wave and an E° of -0.28 V (vs. NHE, Figure 4c). Comparison of the E° and pFe of **1** shows a clear correlation with hexadentate siderophores, providing further evidence that the ADPA group is involved in iron binding (Figure 4c,d; Supporting Information, Table S7).

Together, results from HR-MS, pFe measurements, CV, and UV/Vis absorption spectroscopy are all consistent with a 1:1 Fe^{III}-crochelin A complex, in which iron is bound in a hexadentate fashion. A comparison with results from **4** strongly suggests that the ADPA moiety binds iron via its amino and one of the hydroxy groups. This is entirely in agreement with the expected chemistry of iron ligation by siderophores: the ADPA group can form a favored 5-membered chelate ring via its terminal amine and one of the two hydroxy groups. The pK_a values of the amine and hydroxy groups are in a range similar to those of well-known iron-ligating moieties in other siderophores. When the amine is acylated, as in **2–4**, the pK_a values of the two hydroxy groups are too high to bind Fe^{III} efficiently at neutral pH, thus explaining the lower pFe and differential UV/Vis spectral profiles as a function of pH for the acylated derivative (Figure 4; Supporting Information, Figures S23–25).

Finally, we addressed the biosynthesis of crochelins and the incorporation of the unusual γ -amino acid ADPA using bioinformatics. As alluded to above, of the three siderophore gene clusters in *A. chroococcum*, two are homologous to those of vibrioferrin and amphibactin, leaving one as the

candidate crochelin cluster, which we annotate as *cro* (Figure 1c). This cluster is adjacent to a number of *nif* genes, which are responsible for nitrogen fixation.^[15] The genes in the putative *cro* cluster include non-ribosomal peptide synthetases (NRPSs) and a polyketide synthase (PKS). An examination of the NRPS adenylation (A) domain specificities and the arrangement of the NRPS and PKS genes suggest that crochelins represent the co-linear product of the *cro* cluster (Figure 5). The proposed biosynthesis begins with stepwise incorporation of a fatty acyl group and Ser by CroD, followed by incorporation of malonyl-CoA and reduction of the β -ketone to a hydroxy group to form the ADPA unit by CroE. A similar sequence was previously proposed in the biosynthesis of **5**.^[12] The three remaining NRPSs (CroF–CroH) install β -OH-Asp, Dab, and *N*-formyl-*N*-OH-Orn. How putrescine is condensed to the C-terminus of the peptide remains to be determined.^[15] In strong support of the proposed pathway, we observed each biosynthetic intermediate, that is, the free acid form of the products of CroD, CroE, CroF, both intermediates of CroG, and CroH by HR-HPLC-MS and HR-MS/MS (Figure 5, Supporting Information, Figure S26). These intermediates are presumably released by premature hydrolysis from the NRPS/PKS assembly line.

The *cro* cluster also contains two genes with homology to deacylases (Figure 1c). One of these, *croM*, is highly similar to *pvdQ*, which has been shown to deacylate pyoverdine upon export, a key step in the maturation of the siderophore.^[16] Likewise, CroM could be involved in “activating” crochelin prior to export, by unveiling its terminal amine, which our studies show is important for chelating iron. We suggest that acylation of the ADPA-amine in **1** is a simple strategy by which cells lower the iron affinity inside the cell and facilitate removal of the metal for cellular use, once the holo-side-

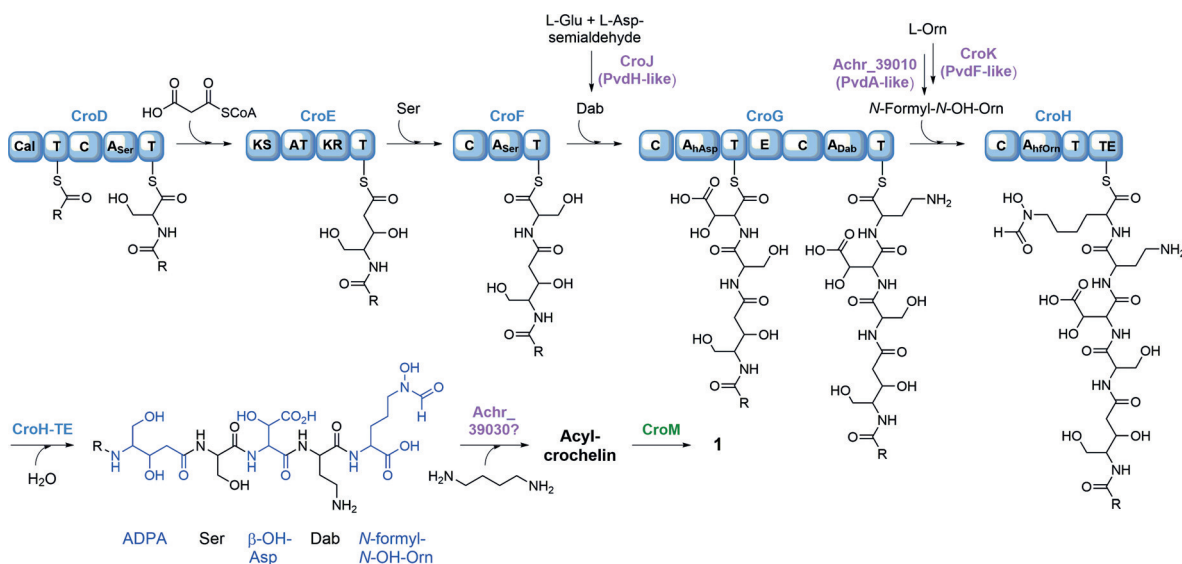


Figure 5. Proposed biosynthesis of crochelins. The acyl-CoA ligase (Cal) and Ser-specific A-domain in CroD generate an acyl-Ser intermediate. CroE condenses malonyl-CoA to the growing peptide, which upon reduction of the β -keto group gives the ADPA moiety. CroJ likely provides Dab. CroK, in conjunction with the PvdA-like hydroxylase, generates *N*-formyl-*N*-OH-Orn. CroFGH append Ser, Dab, and *N*-formyl-*N*-OH-Orn to create the hexapeptide scaffold. A VibH-like protein elsewhere in the chromosome or the A-domain bearing protein near the *cro* cluster (Achr_39030) may be involved in condensation of putrescine.^[15] Hydrolysis of the acyl group by CroM completes the maturation of **1** as confirmed by in vitro analysis with CroM (see Figure 6b).

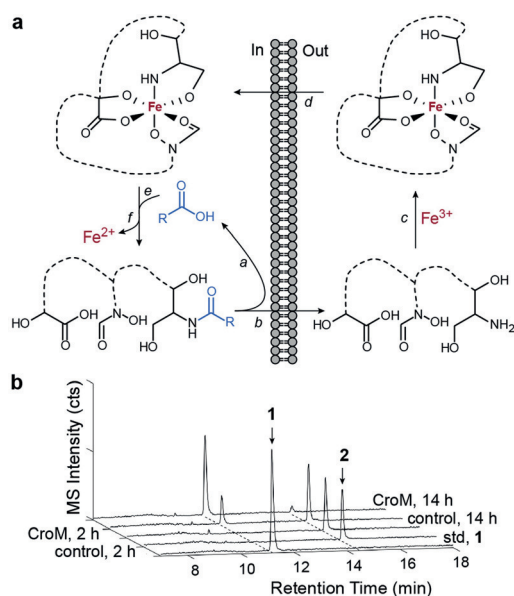


Figure 6. Role of CroM in maturation of **1** and release of iron. a) Upon synthesis of the acylated form, crochelin is “activated” via deacylation by the PvdQ-like CroM and secreted (steps a, b). There, **1** A binds Fe^{III} (step c), the holo-siderophore is re-imported (step d), and acylated to lower its affinity for iron and facilitate release of the bound metal (steps e, f). b) CroM catalyzes deacylation of **2** to **1**. Reactions of CroM with **2** after 2 h and 14 h result in formation of **1**, while controls without CroM do not. Std: standard.

rophore is taken up. Deacylation to **1** could then allow the cycle to start over again, a model that is consistent with the low pFe values we determined for acylated crochelins (Figure 6a). A similar phenomenon has previously been observed with ferrichrome in *E. coli*.^[17] To begin to test this model, we heterologously expressed CroM in *E. coli* (Supporting Information, Table S8). Extraction of the periplasmic component, where this protein is localized,^[16] and reaction with purified **2** and **3** showed accumulation of **1** as a function of time (Figure 6b; Supporting Information, Figure S27). By contrast, the control reaction lacking CroM did not result in any conversion of **2** or **3** into **1**. These results establish the role of CroM in maturation of **1** and at the same time provide experimental support linking the *cro* cluster to crochelin biosynthesis (Figure 5, Figure 6a).

In summary, we report the structure and characterization of crochelin A, the founding member of a new family of siderophores that exhibit hexadentate ligation of Fe^{III} via a hydroxamate, an α -hydroxycarboxylate, and an ADPA group, which bears an α -amino-hydroxy chelating functionality. Bioinformatic analysis of the crochelin gene cluster provides a model for incorporation of the ADPA moiety into the siderophore. Our results afford a mechanism in which prior to export, the acyl group bound to the ADPA-amine is cleaved, which increases the pFe by several orders of magnitude and activates the siderophore for iron chelation outside the cell. The switch in pFe based on acylation of the ADPA-amine suggests a new strategy by which cells can reduce the iron affinity of siderophores inside the periplasm and remove the metal from the holo-siderophore. As a nitro-

gen-fixing bacterium, *A. chroococcum* requires a constant supply of iron to assemble the iron-rich cofactors in nitrogenase. It gains access to iron using three types of siderophores, crochelin A, as well as vibrioferrin and amphibactin. Why it synthesizes **1**, with its unusual ADPA group, and the advantages that it provides relative to vibrioferrin and amphibactin are interesting and yet-unresolved issues.

Acknowledgements

We thank Dr. Kyuho Moon and Leah Bushin for helpful discussions, Prof. Alison Butler for amphibactin standard, as well as the Princeton Environmental Institute Innovative Research Award (to O.B. and M.R.S.), the National Science Foundation (grants OCE 1315200 to F.M.M.M. and EAR 1631814 to X.Z.), and the Pew Biomedical Scholars Program (to M.R.S.) for support of this work.

Conflict of interest

The authors declare no conflict of interest.

Keywords: *Azotobacter chroococcum* · biosynthesis · chelome · natural products · siderophores

How to cite: *Angew. Chem. Int. Ed.* **2018**, *57*, 536–541
Angew. Chem. **2018**, *130*, 545–550

- [1] R. C. Hider, X. L. Kong, *Nat. Prod. Rep.* **2010**, *27*, 637–657.
- [2] I. J. Schalk, M. Hannauer, A. Braud, *Environ. Microbiol.* **2011**, *13*, 2844–2854.
- [3] a) J. H. Crosa, C. T. Walsh, *Microbiol. Mol. Biol. Rev.* **2002**, *66*, 223–249; b) C. T. Walsh, M. A. Fischbach, *J. Am. Chem. Soc.* **2010**, *132*, 2469–2493.
- [4] J.-H. Becking in *The prokaryotes*, Springer, Heidelberg, **1981**, pp. 795–817.
- [5] R. L. Robson, R. Jones, R. M. Robson, A. Schwartz, T. H. Richardson, *PLoS ONE* **2015**, *10*, e0127997.
- [6] a) Y. Bashan, *Biotechnol. Adv.* **1998**, *16*, 729–770; b) J. Mishra, R. Singh, N. K. Arora, in *Probiotics and Plant Health* (Eds.: V. Kumar, M. Kumar, S. Sharma, R. Prasad), Springer Singapore, Singapore, **2017**, pp. 71–111.
- [7] M. V. Martinez Toledo, J. Gonzalez-Lopez, T. de la Rubia, J. Moreno, A. Ramos-Cormenzana, *Biol. Fertil. Soils* **1988**, *6*, 170–173.
- [8] a) A. Verma, K. Kukreja, D. Pathak, S. Suneja, N. Narula, *Indian J. Microbiol.* **2001**, *41*, 305–307; b) M. E. Brown, *Microbiology* **1968**, *53*, 135–144.
- [9] a) O. Baars, F. M. M. Morel, D. H. Perlman, *Anal. Chem.* **2014**, *86*, 11298–11305; b) O. Baars, D. H. Perlman in *Applications from Engineering with MATLAB Concepts* (Ed.: J. Valdmann), InTech, Rijeka, **2016**, pp. 191–214.
- [10] O. Baars, X. Zhang, F. M. Morel, M. R. Seyedsayamdost, *Appl. Environ. Microbiol.* **2015**, *82*, 27–39.
- [11] J. S. Martinez, J. N. Carter-Franklin, E. L. Mann, J. D. Martin, M. G. Haygood, A. Butler, *Proc. Natl. Acad. Sci. USA* **2003**, *100*, 3754–3759.
- [12] A. C. Ross, Y. Xu, L. Lu, R. D. Kersten, Z. Shao, A. M. Al-Suwailam, P. C. Dorrestein, P.-Y. Qian, B. S. Moore, *J. Am. Chem. Soc.* **2013**, *135*, 1155–1162.

- [13] J. Franke, K. Ishida, M. Ishida-Ito, C. Hertweck, *Angew. Chem. Int. Ed.* **2013**, 52, 8271–8275; *Angew. Chem.* **2013**, 125, 8429–8433.
- [14] H. Stephan, S. Freund, W. Beck, G. Jung, J.-M. Meyer, G. Winkelmann, *Biometals* **1993**, 6, 93–100.
- [15] a) T. A. Keating, C. G. Marshall, C. T. Walsh, *Biochemistry* **2000**, 39, 15513–15521; b) M. R. Seyedsayamdost, S. Cleto, G. Carr, H. Vlamakis, M. João Vieira, R. Kolter, J. Clardy, *J. Am. Chem. Soc.* **2012**, 134, 13550–13553.
- [16] E. J. Drake, A. M. Gulick, *ACS Chem. Biol.* **2011**, 6, 1277–1286.
- [17] A. Hartman, V. Braun, *J. Bacteriol.* **1980**, 143, 246–255.
- Manuscript received: September 19, 2017
Revised manuscript received: November 4, 2017
Accepted manuscript online: November 14, 2017
Version of record online: December 8, 2017
-